Characteristics of warm season left-moving supercells over the Highveld of South Africa

Christina G. Liesker[a,*], Liesl L. Dyson[a], Erik H. Becker[b]

[a] Department of Geography, Geoinformatics and Meteorology, University of Pretoria, cnr Lynwood Road and Roper Street, Hatfield, 0002, Private Bag X20, Pretoria, 0028, South Africa

[b] Centre for Climate Research Singapore, Meteorological Service Singapore, 36 Kim Chuan Road, Singapore, 537054

ABSTRACT

A supercell is a type of thunderstorm known to produce severe weather conditions that result in damage to property, injuries, and loss of life. Supercells were previously considered rare in South Africa, however since the implementation of the South African Weather Service's single polarisation S-band Doppler radar network in 2010, numerous cases have been identified. Despite this, there is a lack of research on supercells over South Africa, with very little information on their characteristics specific to the region. The aim of this study is to determine the characteristics of warm season left-moving supercells over the Highveld (Gauteng and Mpumalanga province) of South Africa. This was done using a radar derived database, consisting of 115 left-moving supercells, that occurred during the warm seasons (September to February) of 2010/11 to 2019/20. Left-moving supercells were found to be most common in October and November, peaking in the afternoon between 15:00 and 16:00 South African Standard Time (SAST). A shift in the seasonal distribution was observed, with the most active area over Gauteng in November, moving south-eastwards to the south-eastern parts of Mpumalanga by December. Supercell hotspots were identified over the south-western and eastern Highveld of Gauteng as well as the south-eastern parts of Mpumalanga, of which some areas of occurrence appeared to be influenced by topography. The average track direction was found to be from the south-west, with a southerly shift as the season progressed. On average supercells lasted approximately 1 hour 12 minutes, travelled 49 km and at a speed of 41 kmh^{-1}. Having a better understanding of the characteristics of supercells may provide a heightened awareness of preferred areas and times of occurrence of events, how they travel, how long they last and how fast and far they travel, thereby assisting in producing more accurate forecasts, nowcasts and warnings. More detailed studies are required to understand the influence of topography and the atmospheric conditions on these characteristics.

KEYWORDS

supercell, weather radar, severe thunderstorm, short-term climatology, Highveld, South Africa

Abbreviations: SAST, South African Standard Time; ZAR, South African Rand; SAWS, South African Weather Service; SON, September, October, and November; DJF, December, January, and February.

* Corresponding author.
E-mail addresses: christina.liesker@up.ac.za (C.G. Liesker)

1 Introduction

Supercell thunderstorms are notorious producers of severe weather conditions such as large hail, damaging winds, tornadoes and in some cases flooding (Burgess and Lemon, 1990; Moller et al., 1994; Ray, 1990; Weisman and Klemp, 1986). On the 28th of November 2013, at least 7 supercells contributed to significant hail damage across the Gauteng Province of South Africa (see Fig. 1 for locations), which along with the 11th of November 2013 (also a supercell event day) cost insurance companies ZAR (South African Rand) 2 billion (± US$ 109 million) (Dyson et al., 2021; Liesker, 2021). Other noteworthy events occurred on the 11th and 30th of December 2017, where tornadic supercells over the extreme south-eastern and south-western parts of Gauteng respectively, resulted in significant damage to property and injuries (Kruger et al., 2018; Lekoloane et al., 2021). Supercells were previously considered rare in South Africa (e.g., Admirat et al., 1985; Carte, 1979, 1981; De Coning et al., 2000), however, with the installation of the South African Weather Service's (SAWS) Doppler S-band radar network in 2010, numerous events have been detected (Liesker, 2021).

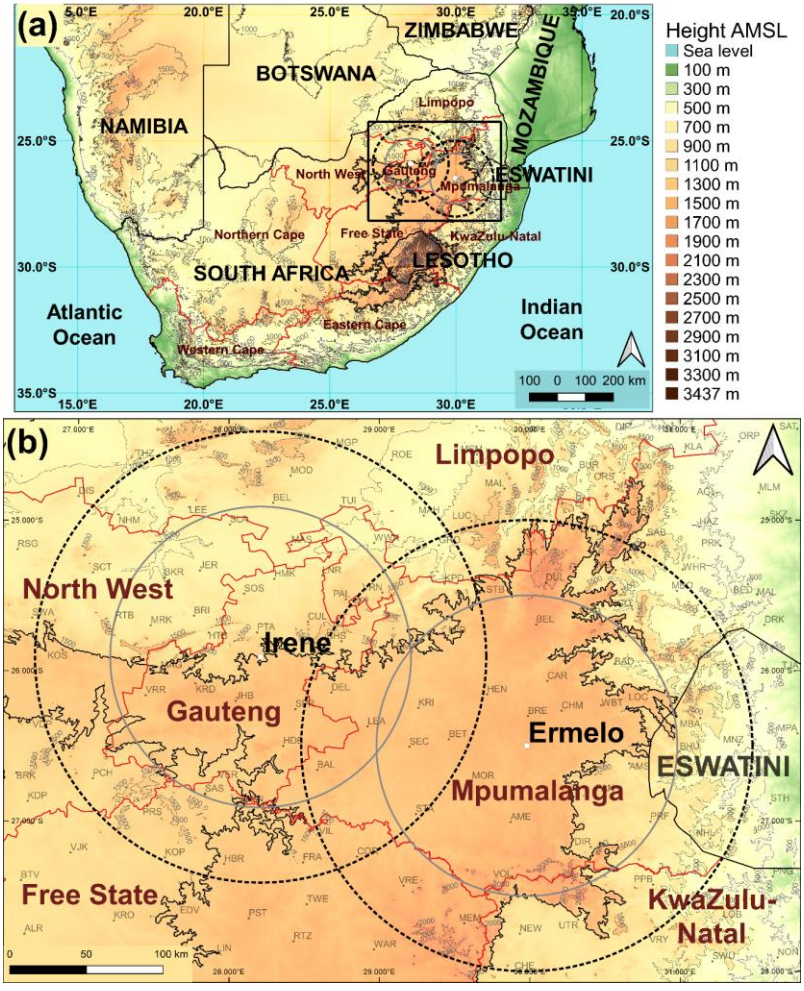

Fig. 1. (a) The location and geographical map of South Africa and (b) the study area. The 150 km (black dotted circle) and 100 km (white circle) range ring from both the Irene and Ermelo radar are shown. The areas of study in this paper are confined to the 100km range rings (white circles) around each radar. Each 500 m AMSL contour is provided in grey and the 1500 m AMSL contour is shown in black indicating the area of the Highveld. (Map created using QGIS, topographical data obtained from: U.S. Geological Survey, 2000).

Supercells are fairly long-lived thunderstorms that contain a deep, and persistent rotating updraft, referred to as a mesocyclone, and remain in a quasi-steady state for an extended period (Browning, 1964; Burgess and Lemon, 1990; Falk, 1997; Moller et al., 1994; Ray, 1990). Such thunderstorms can be identified using

weather radar with recognisable features such as the hook echo and Weak Echo Region (WER) or Bounded Weak Echo Region (BWER) on the reflectivity field (equivalent radar reflectivity factor), as well as a rotational couplet (mesocyclone) on the Doppler velocity field (Browning, 1964; Burgess and Lemon, 1990; Donaldson, 1970; Lemon, 1977; Stumpf et al., 1998). The hook echo is a hook shaped reflectivity echo found in the lower levels of the thunderstorm, the WER is a vertical column of weak radar reflectivity that is bounded by higher reflectivity above and on one side and the BWER is a vertical column of weak radar reflectivity that is bounded by higher reflectivity above and on both sides (in the mid-levels). Rotation of the updraft in a supercell can either be cyclonic (more common) or anticyclonic (less common) and such storms may either deviate to the left or right of the average 0 to 6 km Above Ground Level (AGL) environmental winds (Browning, 1964; Bunkers et al., 2000; Burgess and Lemon, 1990; Moller et al., 1994; Weisman and Klemp, 1984; Wilhelmson and Klemp, 1978). With an environment favouring winds backing with height over South Africa, left-moving supercells[1] dominate, with the clockwise (cyclonic) rotating updraft (mesocyclone) on the rear left flank (Davies-Jones, 1984; Klemp and Wilhelmson, 1978; Liesker, 2021; Weisman and Klemp, 1984). Supercells are found to develop in environments that favour deep moist convection, with strong vertical wind shear (speed and direction) and high instabilities (e.g., Convective Available Potential Energy (CAPE)) (Doswell III and Schultz, 2006; Johns and Doswell III, 1992; Moller et al., 1994; Ray, 1990).

Severe thunderstorms, which produce large hail, damaging winds, tornadoes and/or flooding, are known to frequent South Africa's north-eastern interior, during the spring (September to November (SON)) and summer (December to February (DJF)) season, peaking in November (Admirat et al., 1985; Blamey et al., 2017; Carte and Held, 1978; Dyson et al., 2021; Goliger and Lunt, 1997; Held and Carte, 1979; Olivier, 1990). The Highveld, an elevated area of 1500 m Above Mean Sea Level (AMSL) and greater (enclosed by the black contour on Fig. 1), is particularly prone to severe thunderstorms (Simpson and Dyson, 2018). The north-eastern parts of South Africa experience, on average, high vertical wind shear and CAPE values during the warm season (especially during spring and early summer), contributing to conducive severe thunderstorm environments (Blamey et al., 2017; Dyson et al., 2015; Taszarek et al., 2021). Early in the season vertical wind shear values dominate (peaking in October and November), with predominantly extra-tropical weather systems influencing this region, while CAPE values also increase (Blamey et al., 2017; Dyson et al., 2015). However, later in the summer season, weather systems become more tropical in nature, with a further increase in moisture and CAPE (peaking in December), but a decrease in the vertical wind shear, corresponding to a decrease in severe thunderstorm activity. Dyson et al. (2015) showed that although mid and upper tropospheric temperatures slowly increase during spring, they remain below normal during November and December, while at the same time the surface temperatures increase, resulting in high values of lower tropospheric temperature lapse rates. In addition, the surface moisture increases, with a doubling of the surface dew-point temperatures from October to December. These factors contribute to the peak in CAPE observed during December. Earlier in the summer season surface moisture originates from the east as the surface high pressure systems result in an onshore flow over the interior (Taljaard, 1996), however, in later summer tropical sourced air flows southward.

Research on supercells in South Africa, is limited to a few case based studies (e.g., Carte, 1981; De Coning et al., 2000; Lekoloane et al., 2021; Powell and Burger, 2014) and a study on a modified supercell composite parameter (Rae, 2014), with no research results on their characteristics. Over South Africa, the focus has

[1] A left-moving supercell is defined in this study as a supercell in the Southern Hemisphere that contains a clockwise (cyclonic) rotating updraft on the rear left flank, which tend to deviate to the left of the mean 0 to 6 km environmental winds.

predominantly been on severe thunderstorm climatologies using either visual observations (e.g., Admirat et al., 1985; Carte and Held, 1978; Goliger and Lunt, 1997; Goliger and Retief, 2007; Olivier, 1990) or reanalysis data (e.g., Blamey et al., 2017; Brooks et al., 2003; Dyson et al., 2021; Taszarek et al., 2021), with only a few short term studies using radar data (e.g., Carte, 1979, 1981; Carte and Held, 1978; Mader et al., 1986; Steyn and Bruintjes, 1990). Liesker (2021), created a supercell database (Liesker, 2023) over the Highveld of South Africa (Fig. 1), over 10 spring and summer seasons, using all available radar data to manually identify these cases. This database is open-source and freely available for download.

The aim of this paper is to determine the characteristics of warm season left-moving supercells over the Highveld of South Africa using a 10-year radar-derived supercell database. The database is introduced in this paper and thus we have included a short summary of how it was created, some limitations detecting events as well as a brief overview of the database itself. The spatial, temporal and track characteristics are investigated in this study. A number of similar studies have been conducted in other regions around the world (e.g., Antonescu et al., 2010; Bunkers et al., 2006; Christodoulou and Sioutas, 2017; Feldmann et al., 2021; Hocker and Basara, 2008; Piscitelli et al., 2022; Wapler et al., 2016) and were also based on fairly short time periods, (between 3 and 12 years, except Bunkers et al. (2006) who used events dating back to the 1950's). Preferred areas of development and decay, preferred time of the day and year that they occurred in, lifespan and direction of movement were some of the characteristics investigated by said researchers and their results are compared to ours in section 4. This type of information is useful in better understanding such thunderstorms and together with an understanding of the atmospheric and topographic influences on these characteristics, may assist in more accurate forecasts and warnings. In return this may benefit insurance and other industries impacted by severe weather.

This paper is outlined as follows. Section 2 provides a brief overview of the radar-derived supercell database and methodology used to achieve the aim. This is followed by section 3, which presents the results, section 4, the discussion and then section 5, the conclusion, and recommendations.

2 Data and methodology

The radar-derived supercell database (Liesker, 2021; Liesker, 2023), was used to determine the characteristics of warm season left-moving supercells over the Highveld of South Africa. This database consists of events that occurred from September to February 2010/11 to 2019/20. Although 6 right-moving events were also available within this database, they were not considered in this study due to the low number of events. This database was created using data from the SAWS's Irene and Ermelo S-band Doppler radars, which operate in a single horizontal polarisation, at a maximum radial range of 200 km. These radars cover the north-eastern interior of South Africa (the 150 km range is shown by the dotted circles in Fig. 1) and have a temporal resolution of approximately 6 minutes. (Liesker, 2021)

The supercells, in this database, were identified through a manual process, using both the radar's reflectivity and Doppler velocity field. Fig. 2 provides the decision tree that was used to identify a supercell and is in line with the definition used in other studies (e.g., Antonescu et al., 2010; Bunkers et al., 2006; Hocker and Basara, 2008; Klimowski et al., 2003; Moller et al., 1994). More detailed information regarding the identification of supercell events and the influences on this database can be found in Liesker (2021). Since only left-moving supercells were considered in this paper, the mesocyclone and thus radar features discussed in this section are found on the left flank.

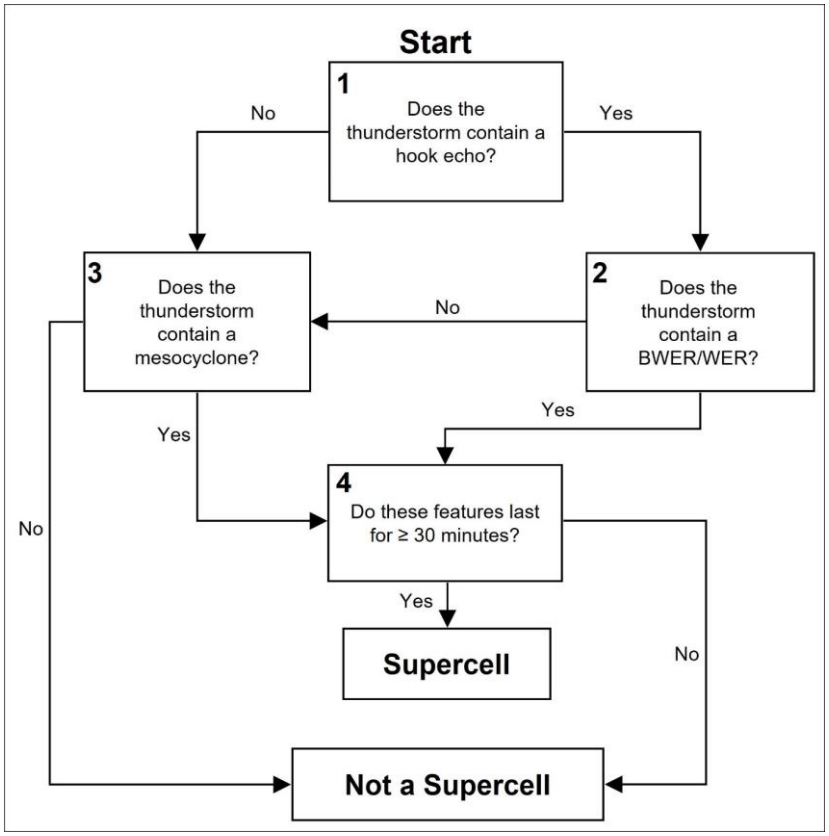

Fig. 2. Supercell identification decision tree using radar data to manually identify events.

The radar's reflectivity field was consulted first when implementing the decision tree. Any thunderstorm that contained high reflectivities (at least 50 dBZ or more), persisted, deviated to the left of the average environmental flow, contained an inflow notch, strong reflectivity gradient on the inflow side of the storm or any other possible indication of a severe thunderstorm, was investigated further. The first criterion considered, to classify a supercell (i.e., criterion 1 on Fig. 2), was if the thunderstorm contained a clear hook echo, pendent shape, or other similar shape, as suggested by Fujita in 1973 cited in Markowski (2002), in the lower levels (2 to 4 km) on the reflectivity field. If the hook echo was present, then a cross-section was taken through the updraft and the presence of a WER and/or BWER was required (criterion 2 on Fig. 2). A BWER region may not necessarily occur throughout the supercell's lifetime (sometimes only in the mature stage) and in some cases it may not be present at all, however, in such cases a persistent WER usually occurs (Burgess and Lemon, 1990; Lemon, 1977; Moller et al., 1994). For this reason, either a WER or BWER was required. The reflectivity features alone (hook echo and BWER/WER) were considered sufficient to classify a thunderstorm as a supercell, which was a similar approach to studies done by for example Bunkers et al. (2006) and Klimowski et al. (2003).

The hook echo may not always be present or well defined. For example, Low Precipitation and High Precipitation supercells may lack the classic hook shape (Bluestein and Woodall, 1990; Burgess and Davies-Jones, 1979; Grant and Van Den Heever, 2014; Moller et al., 1994). Thus, if no clear hook echo (similar shape) or WER/BWER was found to occur, the Doppler velocity field was consulted (criterion 3 on Fig. 2). In such cases the thunderstorm had to contain a mesocyclone between 2 and 8 km AGL with a width between 1 and 10 km. The presence of a mesocyclone alone was considered sufficient to classify it as a supercell. Hocker and Basara (2008), Antonescu et al. (2010) and Feldmann et al. (2021), for example, only used the presence of a mesocyclone on the Doppler velocity field to identify supercells.

The last criterion considered (criterion 4 on Fig. 2), was a time-based criterion. The supercell features identified on radar (reflectivity field and/or Doppler velocity field) had to persist for at least 5 radar scans, which is approximately 30 minutes given the radar's temporal resolution of around 6 minutes. This time criterion was also used by other studies (e.g., Antonescu et al., 2010; Hocker and Basara, 2008) and in line with the supercell definition defined by Moller et al. (1994), who stated that supercells last for 10s of minutes.

The supercell database consists of the centroid position of each supercell, from when a thunderstorm first showed supercell features (supercell initiation) until the last scan where features were found to occur (supercell decay). The Thunderstorm Identification, Tracking Analysis and Nowcasting (TITAN) algorithm (Dixon and Wiener, 1993) was used to obtain these centroid positions. In some cases, however, the TITAN algorithm was not optimal (i.e., more than 1 thunderstorm was tracked) and for such cases, the centroid position was manually obtained. If data was missing for more than 1 radar scan prior to initiation (after the decay) (i.e., more than 12 minutes elapsed between the available scans) the location and time of the initiation (decay) of the supercell was marked as "unknown".

Several limitations impacted the identification of events and thus this database is by no means an exhaustive list of all events. Issues such as the distance from the radar and data availability had a significant impact on event identification. Although each radar has a maximum range of 200 km, due to limitations such as decreasing resolution and height of the radar beam increasing with distance, all events were identified within 150 km from each radar (black dotted circle on Fig. 1), while most events were identified within 100 km (grey circle on Fig. 1) (Liesker, 2021). Beam broadening effects and the effective beamwidth together result in a decrease in the radar's resolution with distance and thus impact the detection of small-scale features (e.g., hook echo and mesocyclone) further away from the radar (Brown et al., 2002; Burgess and Lemon, 1990; Donaldson, 1970; Rauber and Nesbitt, 2018). This may have had the greatest impact on the detection of events beyond 150 km. With most events identified within 100 km, this area was considered the area with the most reliable data.

Radar data availability also played an important role in the ability to identify all events, with either parts of a day, entire days or seasons missing. Overall, the Irene radar had a high data availability, while although the Ermelo radar suffered more outages, availability improved during the 2nd half of the study period (Liesker, 2021). Both radars had a very low availability during the 2012/2013 warm season and thus no supercells were identified in this season (Fig. 3).

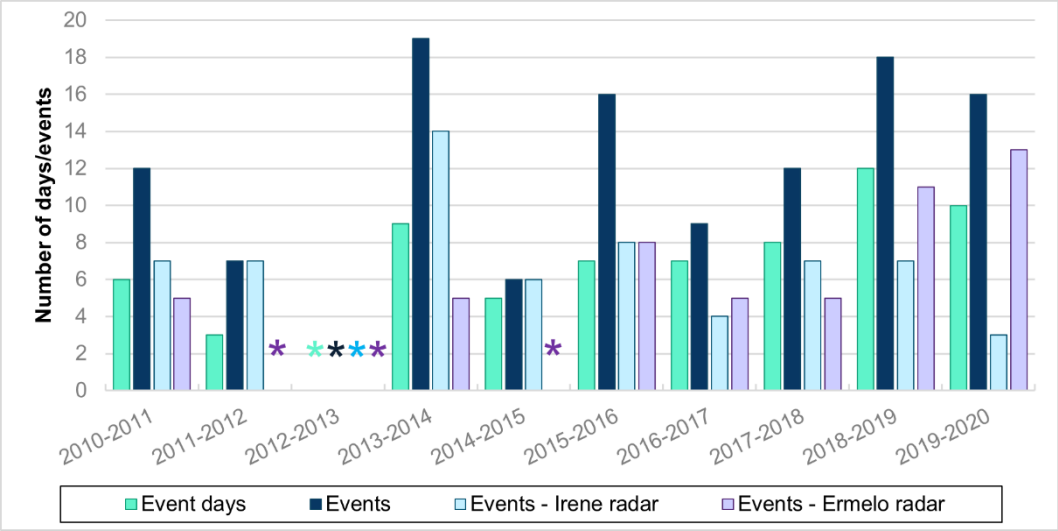

Fig. 3. The warm season (September to February) 2010 to 2020 annual distribution of left-moving supercells. The * indicates where data availability was limited or not available.

Some additional factors may have impacted the detection of the mesocyclone on the Doppler velocity field, including the Nyquist velocity (which was low during certain periods), the location of the feature relative to the radar, as well as the flow dynamics within and around the rotating updraft (Brown and Wood, 2007; Joe and May, 2003). Finally, the subjectivity in the method used to classify events may have resulted in the non-detection of events. The classification was heavily based on the reflectivity field, which was usually consulted first. The velocity field was only consulted if the required reflectivity features were not clear. Thus, if a thunderstorm did not show any typical characteristics indicative of a supercell (e.g., deviation to the left of the average environmental winds), then such events may have been missed. There may have been a bias towards the more severe and classic events (Liesker, 2021).

In total, the database consists of 115 left-moving supercells that occurred on 67 event days (a day on which at least 1 left-moving supercell was found to occur), with an average of 1.8 events per event day. In total 63 events were identified using the Irene radar (predominantly covering the Gauteng Province) and 52 using the Ermelo radar (predominantly covering the Mpumalanga Province) (Fig. 3). On average 7.4 event days and 12.8 events occurred per season. The highest number of events identified on a single day was 7 (28th of November 2013), while 2 event days consisted of 6 events (5th of November 2010 and 16th of November 2015).

This study identified various characteristics of left-moving supercells over the Highveld of South Africa using this supercell database. This included the monthly, diurnal, and spatial distribution as well as the track direction, duration, distance, and speed. It is important to note that these characteristics are based on the available database, which may not contain all events. In addition, the study period, although covered 10 warm seasons, only consisted of supercells identified in 9 of these seasons (excluding 2012/2013), thus these characteristics are only representative of a short-term climatology. However, the length of our study period

is similar to other studies in other regions around the world (e.g., Antonescu et al., 2010; Christodoulou and Sioutas, 2017; Feldmann et al., 2021; Hocker and Basara, 2008).

The limitation of data availability was taken into consideration when analysing the monthly averages for the supercell events and event days. Where a full day of data was missing for more than half the analysed period, it was removed from the average number calculation. For example, both radars did not have available data from September until December 2012, thus these periods were excluded from the averages calculated for the entire study area. When looking at the averages identified by each radar, the availability had a greater impact on the Ermelo radar (Liesker, 2021).

Quantum Geographic Information System (QGIS) was used to display the tracks and help analyse the data. The track was created by converting the centroid position at each time step to a vector line for each event. The distance for each track was then calculated using the QGIS length function. The supercell direction was calculated using the initiation and decay centroid position (latitude and longitude) of each supercell. The duration was calculated from the time of initiation to the time of the decay while the average speed was calculated using the distance (calculated in QGIS) as well as the duration that the supercell lasted.

It is important to note that the thunderstorm itself may have lasted for some time prior to (after) the supercell features developing (decaying). In addition, the time/location of initiation (decay) may not be the exact time/location that a supercell developed (decayed), as it is dependent on the time the scan was available. Features may have developed (decayed) at any time during the 6-minute period prior to the first scan (after the last scan) containing supercell features. On 4 occasions the initiation and/or decay was unknown and thus these events were excluded from the diurnal distribution as well as the statistics relating to the distance, duration, and speed. However, these events were included when calculating the direction that the supercell travelled, as the impact on direction was low.

The spatial distribution of all the left-moving supercell tracks was analysed using a Kernel Density Estimation (KDE) function. A similar approach to that used by Hocker and Basara (2008) was adopted, although some adjustments were made. Supercell tracks were not buffered to incorporate their swath thus, it was based purely on their vector path, which in turn was based on the centroid position, and not their area of influence. Considering the characteristics of supercells is still largely unknown within this region, an appropriate value to account for the variation in the size of events is not known. A grid of 1 km by 1 km was created over the data area containing the supercell tracks, which was a slightly smaller grid than that used by Hocker and Basara (2008), as our study area and database was smaller. The number of lines that occurred within a 10 km search radius from each 1 km by 1 km grid cell was identified. The entire line was used, not the individual segments (between each centroid position). A KDE analysis was only done on the supercell tracks and not the initiation and decay locations, due to the limited dataset.

3 Results

3.1 Diurnal distribution

The diurnal distribution for the initiation and decay times of left-moving supercells increases from 11:00 South African Standard Time (SAST) onwards, with the initiation peaking at 15:00 SAST and the decay at 16:00 SAST (Fig. 4). Most events (88%) developed between 13:00 and 19:00 SAST and decayed between 14:00 and 20:00 SAST. A decrease in activity is observed by the evening with very few events developing or decaying overnight and during the early morning hours.

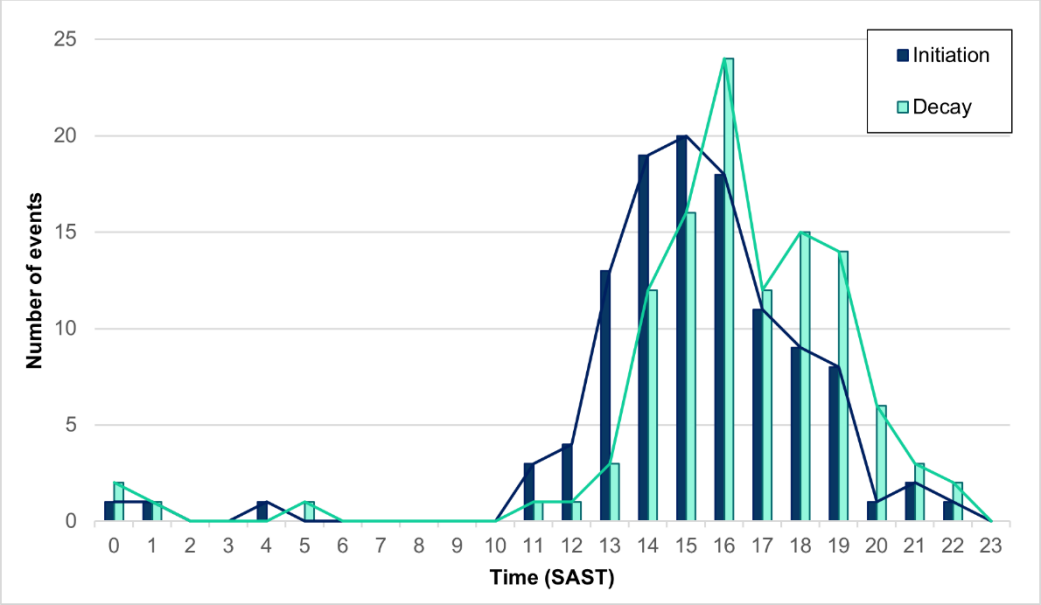

Fig. 4. The diurnal distribution of supercell initiation (dark blue) and decay (cyan) for all events with known initiation and decay times identified within the study period. The times were categorised into hourly intervals in SAST.

3.2 Seasonal distribution

Considering both radars together, there is an increase in left-moving supercell event days and events (number and average) during spring (SON) and a decrease through the summer months (DJF) (Fig. 5a). Approximately 60% of the event days and 67% of the events occurred during the spring season. The monthly distribution in Fig. 5a shows that the peak in frequency of the event days occurs in October and November, which have the same number of event days, while the peak in the number of events occurs in November. There are 3 days on which 6 or 7 events occurred and all these were in November, contributing to the higher number of events observed during this month.

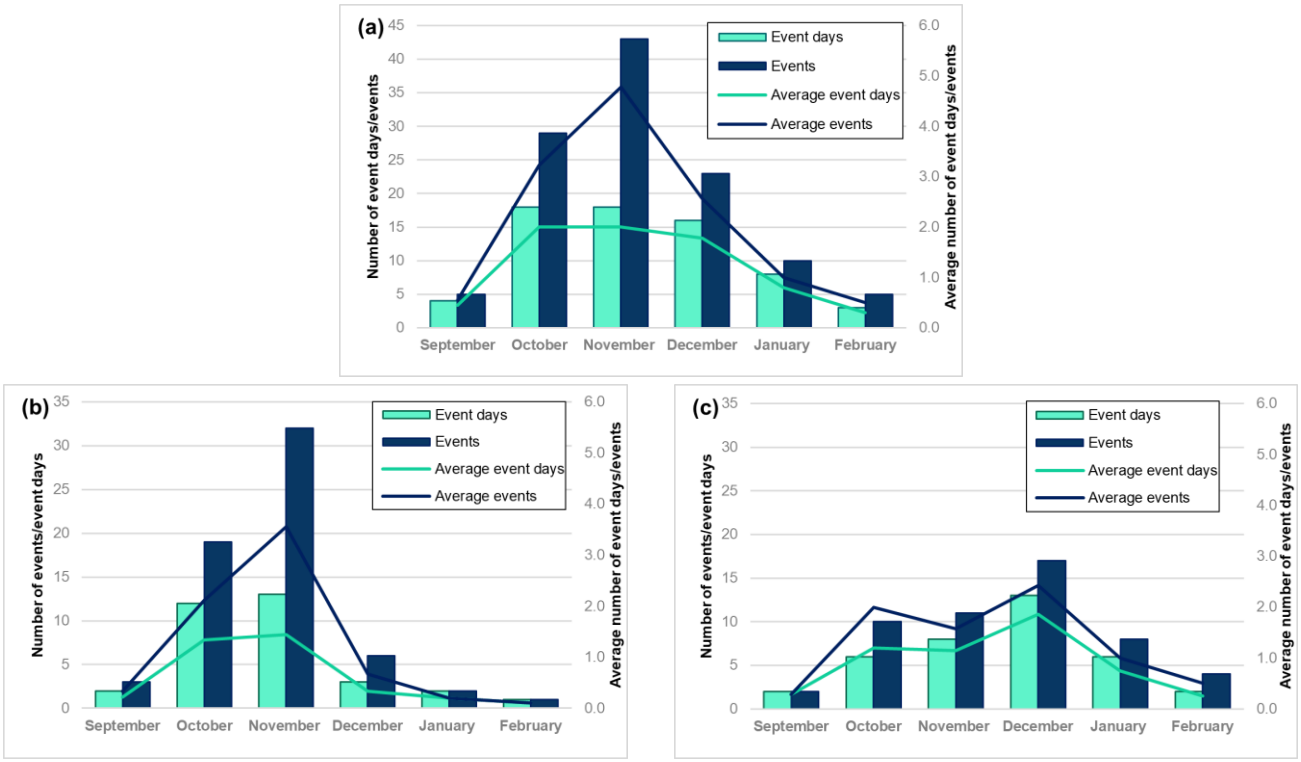

Fig. 5. The monthly distribution for the event days and events over (a) the entire study area (b) Gauteng (Irene radar), and (c) Mpumalanga (Ermelo radar). The bar graph provides the total number (corresponding to the left axis), and the line graph is the average number (corresponding to the right axis).

The seasonal variability of events differs slightly between Gauteng (Irene radar) and Mpumalanga (Ermelo radar). Over Gauteng, supercell event days and events (Fig. 5b) both peak in November (although October only has 1 less event day). In contrast over Mpumalanga the highest number of event days and events occurs during December (Fig. 5c), thus there is an apparent eastward shift in activity as the warm season progresses. In general, supercell activity was higher over Mpumalanga during DJF compared to Gauteng. A secondary peak in the average number of events occurs over Mpumalanga in October (solid blue line in Fig. 5c) however, this is not the case when looking at the total number of events with November containing 1 more event compared to October (Fig. 5c).

We investigated the impact of data availability on the monthly distribution, by considering all the months for only the last 5 seasons. These all had a high data availability. The seasonal distribution for Gauteng and Mpumalanga was similar to the results presented in Fig. 5 b and c. Over Mpumalanga, the same peak in the average event days and events occurs in December, with DJF having more events than SON and more events compared to Gauteng. In addition, the slight peak in average events in October is also observed, while November no longer had a slightly higher number of events compared to October.

Further evidence on the eastward shift in supercell distribution as the season progresses, is present in Fig. 6. Early in the season (September), supercells are confined to the southern Highveld, spreading north, and increasing in number by October and into November (Fig. 6a). Supercell activity decreases over Gauteng in the summer months (DJF), while the area of higher activity shifts to the south-eastern parts of Mpumalanga during this period (Fig. 6b).

3.3 Spatial distribution

Left-moving supercell tracks are spread throughout Gauteng and Mpumalanga, with hotspots over the south-western (highest activity) and eastern Highveld of Gauteng (area 1 and 2 on Fig. 7a) as well as the

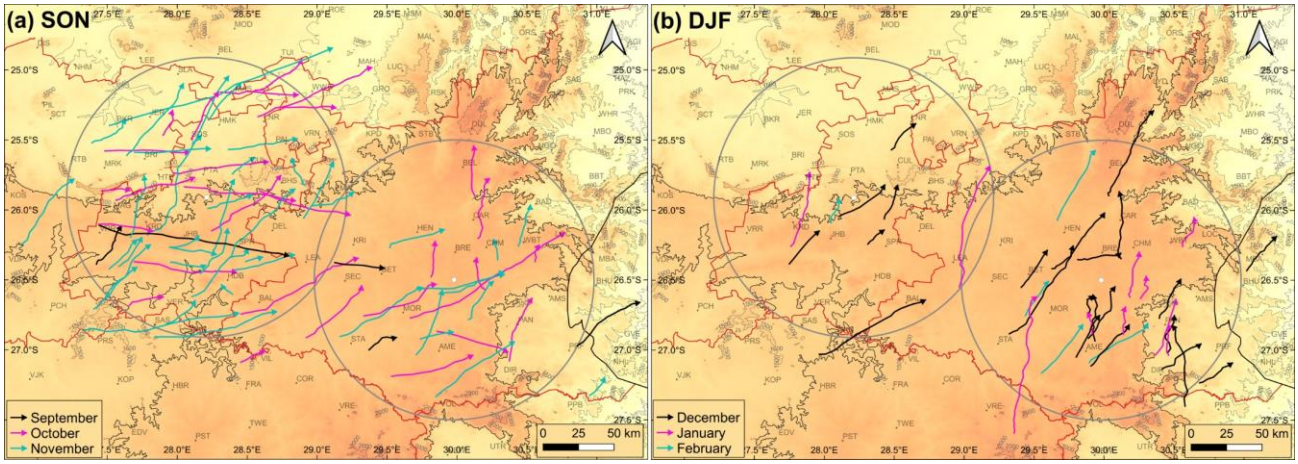

Fig. 6. All Left-moving supercell tracks during the warm seasons of 2010 to 2020 that occurred in (a) September, October, and November (SON), and (b) December, January, and February (DJF).

south-eastern parts of Mpumalanga (area 5, 6 and 7 on Fig. 7c). There were two instances where 2 supercells developed in almost the same location, on separate occasions, over the south-western parts of Gauteng (marked A and B on Fig. 7b). Some moderate activity areas are also noted over the northern parts of Gauteng (area 3 and 4 on Fig. 7a) and western Highveld of Mpumalanga (area 8 on Fig. 7c).

Some of the supercell hotspot and moderate activity areas were noted to occur in areas of complex topography. Several supercells developed along a ridge over south-western Gauteng (Ridge 1 on Fig. 7b), then move north and decay along a ridge to the north (Ridge 2 on Fig. 7b). Most of the supercells decayed on the lee side (relative to the surface wind which was predominantly north-easterly for these cases), however some also decayed on the windward side. Similarly, events developed along Ridge 2 and of those that moved north, most decayed along the Magaliesberg Mountain range (Fig. 7b). In the area of moderate activity east of the Irene radar (area 3 on Fig. 7a), events either moved along the edge of the Highveld (area C on Fig. 7b) or decayed soon after moving off the Highveld. A similar observation is made over the eastern parts of Mpumalanga (area D and E on Fig. 7d), with events decaying soon after moving off the Highveld. Finally, in area 7 (Fig. 7c), located just east of the Highveld edge of Mpumalanga in lower elevation (area E on Fig. 7d), several events developed over the southern parts then moved north, decaying over a similar area, just before the edge of the Highveld. Only one event, which also developed more north compared to the others, was able to move onto the Highveld, but lost supercell features soon after.

In contrast to the above observation, no obvious topographical features contribute to the hotspots in activity observed over the eastern Highveld of Gauteng (area 2 on Fig. 7a), where the busiest airport in Africa (Oliver Tambo International Airport) is located, the south-eastern highveld of Mpumalanga (areas 5 and 6 on Fig. 7c), or in the moderate activity areas north of the Magaliesberg Mountain range (area 4 on Fig. 7a) and west

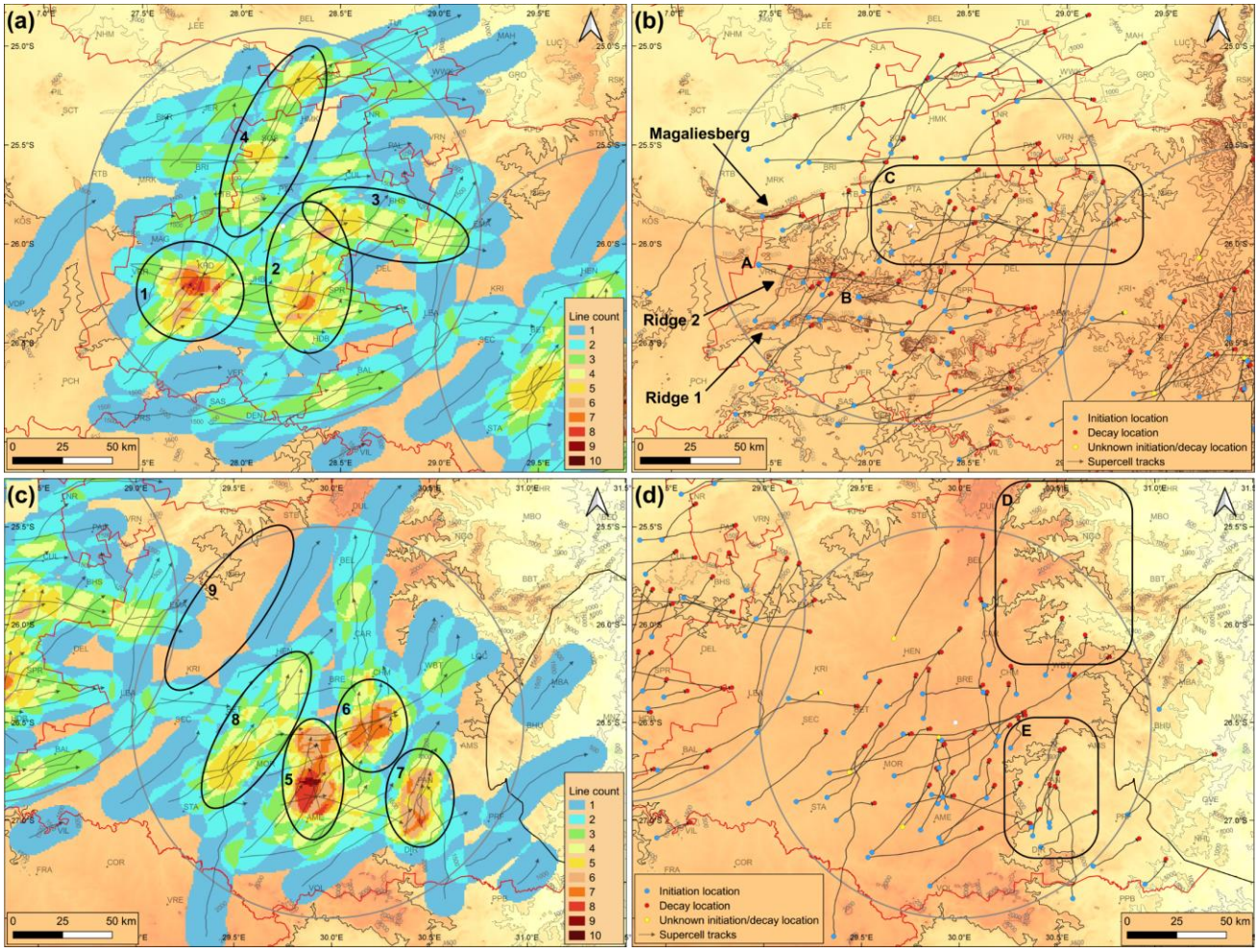

Fig. 7. The track distribution as well as the location of the initiation, decay, and track of all supercells within the warm seasons of 2010 to 2020 over (a and b) Gauteng and (c and d) Mpumalanga. The colours on (a) and (c) indicate the number of tracks that occurred within a 10 km search radius for each 1km by 1km grid point. Figure (b) also includes the 1500 to 1800 m AMSL contours in 50 m intervals to highlight the ridges over Gauteng.

of the Ermelo radar (area 8 on Fig. 7c). All these areas have relatively flat terrain, although influences from nearby ridges, mountain ranges or other topographical features, such as hills, cannot be excluded (not dealt with in detail in this study).

An area of low to no supercell activity is observed north-west of the Ermelo radar (area 9 on Fig. 7c). This region falls within the 100 km radius of the Ermelo radar, thus limitations due to resolution or height of the radar beam are less likely a reason for this area of low activity. This area is also found to occur in a relatively flat region of the Highveld (Fig. 7d), thus no obvious topographical features are noted to be the cause for the low activity.

3.4 Track direction

Considering both radars together, left-moving supercells, over the Highveld of South Africa, were predominantly found to travel from the south-west to the north-east (average direction 224°). Most events travelled from the south-west (29 events) and south south-west (28), while very few travelled from the west north-west (2), south-east (1) and south south-east (2) (Fig. 8). A monthly shift in the supercell track direction is also observed (Fig. 8 and also seen in Fig. 6). In September and October most events travelled from the west and south-west, shifting to a more dominant south-west direction in November and

December and then with a more southerly component by January. In February, a slightly more westerly component is observed again, with most events travelling from the south south-west.

3.5 Duration, distance, and speed

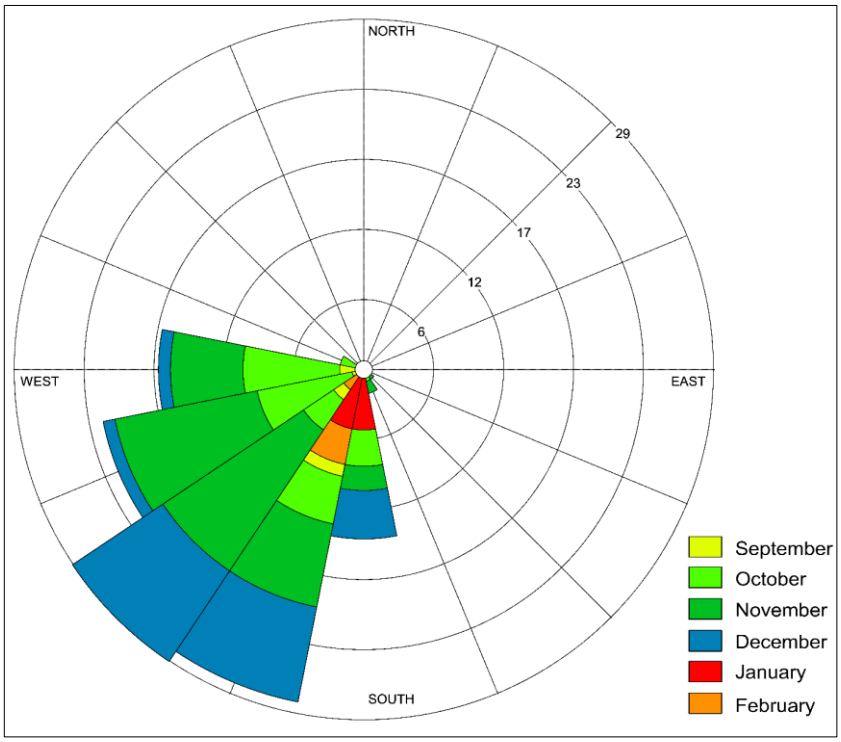

Fig. 8. A rose diagram depicting the number of left-moving supercells track directions in the direction they are travelling from using 16 bins (at 22.5° intervals). The colours indicate the number of events that occurred for each month for a given direction. (Created using WRPLOT View™)

The average lifespan of left-moving supercells over the Highveld of South Africa was approximately 1 hour 12 minutes, their average displacement 48.7 km and average speed 40.8 kmh^{-1}. Most events (75%) lasted between ±30 minutes and 1 hour 30 minutes (Fig. 9a), travelled between 10.8 and 60.4 km (Fig. 9c) and at an average speed of between 17.7 and 48.96 kmh^{-1} (Fig. 9e). The number of events decreased with an increase in lifespan, distance, and speed. In addition, as the lifespan increased the distance covered also increased, however, the longest-lived event was not the longest tracked event and thus also not the fastest event. A similar result was also noted by Bunkers et al. (2006), for supercells in the USA. The longest-lived event lasted 3 hours and occurred on the 16th of November 2015 (A on Fig. 9b), while the longest tracked event occurred on the 1st of November 2018, tracking 172.9 km (B on Fig. 9d). This longest tracked event may have lived longer and therefore also tracked further, as it moved out of the 100 km range of the radar and thus may have been impacted by limitations on the distance from the radar. The fastest moving event occurred on the 10th of October 2010, with an average speed of 83.8 kmh^{-1} (C on Fig. 9f). The top 3 fastest events, with speeds greater than 71 kmh^{-1} (C, D and E on Fig. 9f), all lasted less than ±42 minutes (Fig. 9d), however, other fast-moving events were found to last much longer, thus no significant association between speed of movement and lifespan can be drawn from this. It is important to emphasise once again that the duration, distance, and thus also the speed, are based on the time supercell features were observed on the radar and not the entire lifespan of the thunderstorm.

The lifespan of left-moving supercells over the Highveld of South Africa were also categorised as either short-lived, moderate-lived, or long-lived based on the categorisation used by Bunkers et al. (2006). Most

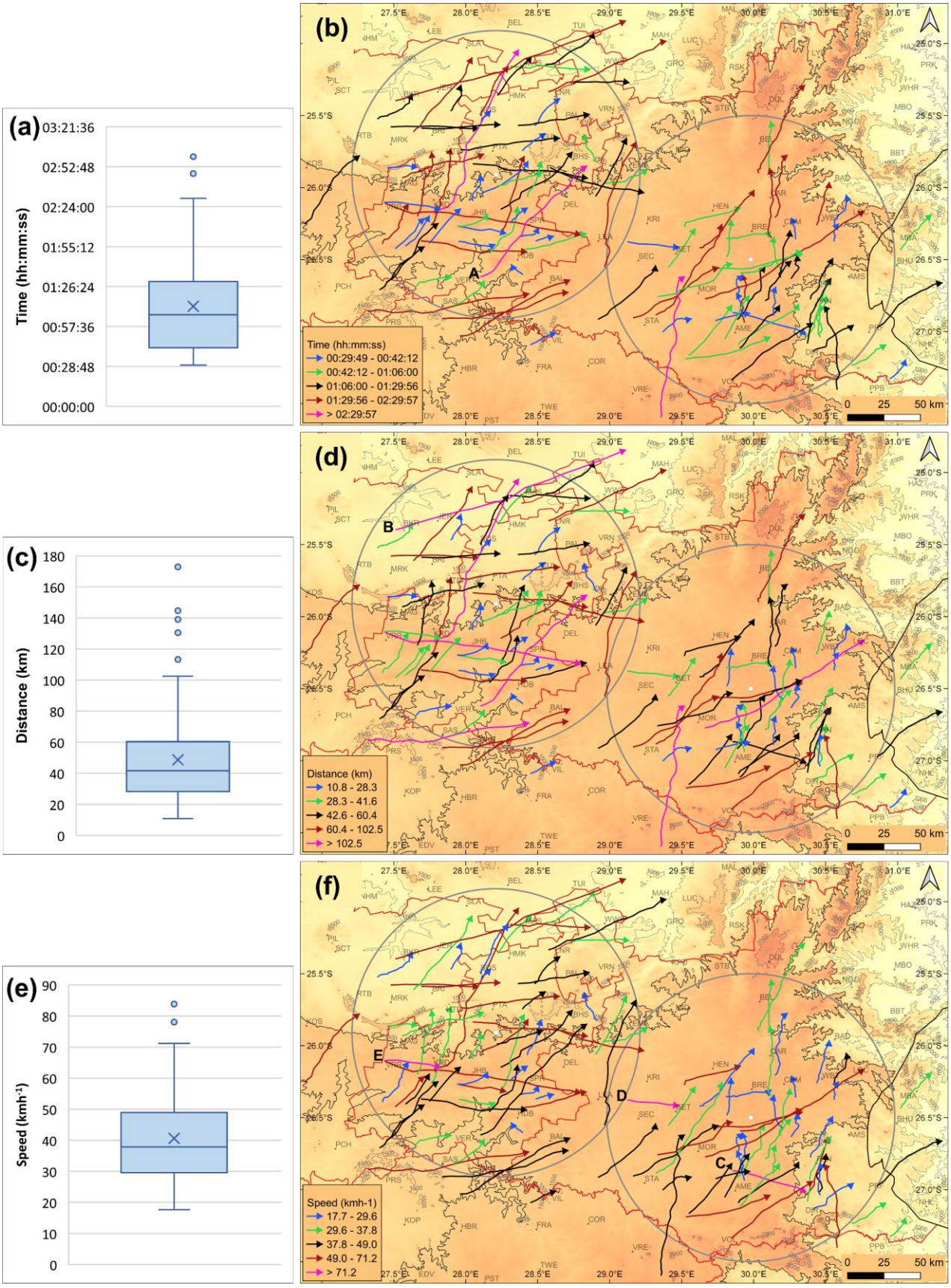

Fig. 9. A box plot showing the spread of the (a) duration, (c) distance tracked and (e) speed of all left-moving supercells as well as the tracks of all events with their (b) duration, (d) distance and (f) speed categorised in 5 groups based on their respective box plots and includes the lower whisker (blue), 1st quartile to median (green), median to 3rd quartile (grey), upper whisker (pink) and outliers (red).

events (88%) were found to be short-lived (lasting ≤ 2 hours), while the rest (12%) were moderate-lived

(lasting >2 hours but < 4 hours). No long-lived events (lasting ≥ 4 hours) were identified.

4 Discussion

The temporal and monthly supercell distribution and peak corresponds well to that of supercells in other regions around the world and severe thunderstorm activity over South Africa. The mid to late afternoon peak in supercell activity was also observed in, for example, the USA (Bunkers et al., 2006; Hocker and Basara, 2008), Romania (Antonescu et al., 2010), central Europe (Germany) (Wapler et al., 2016) and Switzerland (Feldmann et al., 2021), which is the time of maximum diurnal heating. A peak in thunderstorm and hailstorm activity also occurs during the late afternoon over South Africa, although the peak in hailstorm activity (between 17:00 and 18:00 SAST) corresponds to the peak in supercell decay rather than initiation (Admirat et al., 1985; Olivier, 1990; Steyn and Bruintjes, 1990). However, hailstones can still be fairly large during the collapse stage of a supercell (Burgess and Lemon, 1990; Lemon, 1977). The lack of supercell activity during the morning hours was also noted by Olivier (1990), to occur in hailstorm activity over the Highveld of South Africa, while supercells in the USA, Romania, Central Europe, Switzerland and Argentina, also had a minimum during the early to mid-hours of the morning (Antonescu et al., 2010; Bunkers et al., 2006; Feldmann et al., 2021; Hocker and Basara, 2008; Piscitelli et al., 2022; Wapler et al., 2016).

Our results show that spring and early summer months had a peak in the occurrence of supercells, which corresponds to results in, for example, the USA, Romania, Greece and Argentina (e.g., Antonescu et al., 2010; Christodoulou and Sioutas, 2017; Hocker and Basara, 2008; Piscitelli et al., 2022) as well as severe thunderstorm activity over the Highveld of South Africa (e.g., Admirat et al., 1985; Carte and Held, 1978; Dyson et al., 2021; Goliger and Lunt, 1997; Held and Carte, 1979; Olivier, 1990). Blamey et al. (2017) showed that the interior of South Africa had a higher potential for severe convective environments during the early summer months, with the peak also occurring in November. The atmosphere is conditionally unstable with high values of vertical wind shear (speed and direction) during the spring and early summer months, thus contributing to the increase in supercells observed during this period (Blamey et al., 2017; Dyson et al., 2021; Taszarek et al., 2021). Vertical wind shear (speed and direction), especially in the low and mid-levels, was found to be the most important parameter with regards to supercell development (Johns and Doswell III, 1992; Moller et al., 1994). During spring, extratropical weather systems influence the region with a high frequency of cut-off lows and upper-level westerly baroclinic disturbances, coupled with the sub-tropical jet stream (Dyson et al., 2015; Singleton and Reason, 2007; Tyson and Preston-Whyte, 2000). Ridging surface high pressure systems are also found to increase in frequency during spring, transporting moisture over the eastern interior (Ndarana et al., 2022; Taljaard, 1996; Tyson et al., 1996; Tyson and Preston-Whyte, 2000). The combination of these weather systems is known to result in favourable conditions not only for convection (Tyson and Preston-Whyte, 2000) but also severe convection over this region. However, a more detailed study on the presence and interaction of the surface and upper weather systems during severe convective weather (including supercell days) is required. The decrease in supercell activity during the later summer months corresponds to the decrease in vertical wind shear observed over this region, despite high CAPE values still observed (Blamey et al., 2017; Dyson et al., 2015). This is attributed to the southward migration of the sub-tropical jet stream and an increase in tropical weather systems influencing the region.

Drylines over the interior of South Africa have been found to be associated with convective development and linked to several severe convective events (De Coning and Adam, 2000; De Coning et al., 2000; Howard and Washington, 2019; Lekoloane et al., 2021; Van Schalkwyk et al., 2022; Van Schalkwyk et al., 2023). Van Schalkwyk et al. (2022), found that drylines over the eastern interior peak in November, as the north-easterly moisture flux increases, then shift westward later in the summer season. They also suggested that

the ridging high in the east and surface heat trough in the west were responsible for most drylines over the interior of South Africa. Given the November peak in drylines over and just to the west of our study area, they may play an important role in the observed monthly as well as spatial distribution of supercells over this region however, further studies are required to determine if such associations exist.

The south-easterly shift in supercell distribution from, Gauteng to Mpumalanga, corresponds to the seasonal shift in the number of potentially severe convective days identified by Blamey et al. (2017) but does not correspond to the westward shift of hailstorms identified by Dyson et al. (2021) and Olivier (1990). However, not all hailstorms occur from supercells. Vertical wind shear (speed and direction) becomes less favourable over Gauteng in December and January but remains over Mpumalanga, thus likely contributing to this shift in supercell activity.

Left-moving supercell distribution over the Highveld of South Africa corresponds well with areas of tornado observations, hailstorms, and severe thunderstorm environments over this region. Especially over the highly populated areas of Gauteng, similar hotspots in tornado activity were observed by Goliger and Lunt (1997). Dyson et al. (2021) and Olivier (1990) found that hail day frequency was generally high over the southern Highveld of both provinces, however a lower hail day frequency was found to occur over south-eastern Mpumalanga, where we identified a hotspot in supercells. Goliger and Lunt (1997), also identified a lower number of tornadoes over south-eastern Mpumalanga, although observations may be unrepresentative due to the low population in the region. In contrast to this, Blamey et al. (2017) identified the same region as having a large number of potentially severe convective environments, corresponding to our observations. Some other disparities with severe thunderstorm distributions were also observed. Supercell activity was low over the south-western parts of Mpumalanga, despite a high hailstorm activity (e.g., Dyson et al., 2021; Olivier, 1990), although distance from the radar may have influenced the detection of several events in this region. In addition, the total and average number of potentially severe convective environments was low over the south-western parts of Gauteng (Blamey et al., 2017) where supercell activity was high, however, topography appeared to play a significant role in this region.

Supercell initiation, decay, distribution, and track appear to have an apparent link to the complex topography over various parts of Gauteng and Mpumalanga, similar to other studies on supercells around the world (e.g., Bunkers et al., 2006; Christodoulou and Sioutas, 2017; Feldmann et al., 2021; Hocker and Basara, 2008; Mulholland et al., 2018). Several thunderstorms encountered a ridge over the south-western parts of Gauteng developed into supercells, which is in line with Feldmann et al. (2021), who found that mesocyclones tend to develop in storms moving uphill. Supercells were also found to decay along the lee of the ridges over south-western Gauteng (relative to the surface wind), while numerous events also decayed when moving off the eastern Highveld of Gauteng and Mpumalanga. Markowski (2002), noted a weakening of supercells on the lee of a slope (relative to the surface winds) or when moving down into a valley. However, Prociv (2012) found that where supercells encountered a downslope area vorticity stretching and thus strengthening of the low-level rotation could also occur.

The average south-west to north-east track direction of supercells, found in this paper, corresponds to the average track direction of thunderstorms over Gauteng, determined by Mader et al. (1986), which was noted by Steyn and Bruintjes (1990) to have a bias towards more severe events. It also corresponds to the average supercell direction determined in the USA, Greece, and Romania (Antonescu et al., 2010; Bunkers et al., 2006; Christodoulou and Sioutas, 2017; Hocker and Basara, 2008), although a track from the north-west to south-east was also fairly common in those regions and absent in our findings. According to Hocker and Basara (2008), the synoptic conditions and thus average 0 to 6 km AGL winds play a significant role in the

observed track direction. The average 0 to 6 km AGL wind direction for summer in the study area is close to 265° (i.e., westerly) and as anticipated, left-moving supercells had an average track direction slightly to the left of this.

Hocker and Basara (2008), also noted a shift in the supercell track direction over Oklahoma (USA) as the season progressed, similar to the results identified in the findings presented in this paper. The track direction of supercells over the Highveld has a southerly change later in the season, corresponding to the southerly shift in the average monthly 0 to 6 km AGL wind direction.

On average Highveld supercells last for just over one hour well within the 1 to 2 hour range of supercells observed in the USA (Bunkers et al., 2006; Hocker and Basara, 2008) and Romania (Antonescu et al., 2010), with most events lasting between 30 minutes and 1 hour 30 minutes and a decrease in the number of events as the lifespan increased. The average supercell lifespan, determined in our study, was also much longer than the typical lifespan of a thunderstorm over the Highveld of South Africa, which was shown to last on average 30 minutes (Mader et al., 1986; Steyn and Bruintjes, 1990).

Only a few moderate-lived events (12% of the total number) and no long-lived events were identified in the presented results. This differs to the results seen in the USA, Romania, and Greece (Antonescu et al., 2010; Bunkers et al., 2006; Christodoulou and Sioutas, 2017; Hocker and Basara, 2008), where some events were found to last between 5 and 7 hours. Our results show that the longest-lived event was 3 hours. Limitations relating to the radar (e.g., resolution and coverage) may have contributed to the lack of long-lived events identified over the Highveld of South Africa, as 4 moderate-lived events tracked beyond the 100 km range from the radar, thus may have lived longer. Other factors such as topography and environment may also have contributed to the lack of long-lived events, and possibly even the low number of moderate-lived events, as was noted by Bunkers et al. (2006) for the low number of long-lived events in parts of the USA.

Mader et al. (1986) and (Steyn and Bruintjes, 1990), found that thunderstorms over the Highveld travelled on average 8 km and moved with a speed of between 27-30.6 km^{-1}. The average distance travelled by left-moving supercells in our study was much further at 49 km and the average speed 41 km^{-1}. Mader et al. (1986) noted that only 20% of the thunderstorms over the Highveld of Gauteng travelled at speeds greater than 40 kmh^{-1}. However, the average distance and speed of supercells over the Highveld of South Africa, was found to be shorter and slower than supercells over Greece as was determined by Christodoulou and Sioutas (2017), although their study included the entire thunderstorm and not only the period where supercell features were observed.

5 Conclusions and recommendations

The characteristics of left-moving supercells, over the Highveld of South Africa, was determined using a radar-derived database of 115 events that occurred during the warm seasons of 2010/11 to 2019/20. Considering the lack of research on supercells over South Africa in the past, this study has provided new insight into some of the characteristics of such thunderstorms. This information may be able to assist in the forecasting, nowcasting and warning of supercells within this region by providing more information about the time of day, month, and location they most often occur (including areas of common initiation and decay), as well as their typical direction of travel (both overall as well as month to month), longevity, distance of travel and how fast they move. This may help a forecaster to anticipate and better understand such events. With further research on what influences some of these characteristics, forecast/nowcast of such events may also improve. Some of this information (for example, the spatial distribution) may also be useful to industries that are impacted by severe weather.

Although a link between both the topography and severe thunderstorm environments on the temporal and spatial characteristics of supercells was established in some areas, a more detailed study investigating these influences are required. This should include investigating why higher supercell activity occurs over Gauteng compared to Mpumalanga during November and the higher activity over Mpumalanga during DJF compared to SON. It should also include the impact of topography and environment on the movement and lifespan (duration, distance, and speed) on Highveld supercells. In general, a more detailed study of the terrain is required, to establish if any smaller features, such as hills, influenced supercell activity in areas with seemingly flat terrain. A more detailed analysis on the environment (including the synoptic weather systems and mesoscale dynamics (including drylines) that occurred on each supercell event day also needs to be conducted.

Finally, the work done in this study, also needs to be expanded to include other regions in South Africa that fall within the radar network. This would help to gain a better understanding of the supercell characteristics over the entire country. However, it would first require the establishment of a supercell database for these areas. This process will be greatly facilitated by an objective and automatic mesoscale detecting system. Although an automatic mesocyclone detection algorithm was developed in the 80s (Zrnić et al., 1985) and has since been enhanced and used in nowcasting and research around the world, this algorithm has not yet been tested or implemented in South Africa. Testing, enhancing, and implementing a mesocyclone detection algorithm will not only assist in nowcasting supercells but also help expand the database to the entire Doppler radar network over South Africa (reducing the manual work involved) and possibly help to improve the current database by identifying additional cases.

There are some limitations to this research, the most important of which is the short study period and relatively low number of events making a thorough climatology impossible. It is encouraging that our results were found to agree well with literature on severe thunderstorms over South Africa, and supercells in other regions around the world. The other limitations worth noting are the distance from the radar and radar data availability, both which may have impacted our results. It highlights the importance of having a functional, high quality radar network, with each radar located close enough together to be able to adequately detect supercell and other small-scale severe thunderstorm features.

Acknowledgements

We would like to thank the South African Weather Service for the radar data that was used to create the radar-derived supercell database used in this study. Also thank you to Lourens Snyman (from the Department of Geography, Geoinformatics and Meteorology at the University of Pretoria), for helping to create the KDE map and for all his assistance and advice regarding the maps created in QGIS. Finally, thank you to James Ladue from the National Oceanic and Atmospheric Administration for his advice on supercell event identification in the database, especially the more challenging cases.

Declaration of Competing Interest

The authors declare that they have no known competing financial interests or personal relationships that could have appeared to influence the work reported in this paper.

Funding sources

This research did not receive any specific grant from funding agencies in the public, commercial, or not-for-profit sectors.

Data availability

The dataset related to this article can be found at https://doi.org/10.25403/UPresearchdata.23617092.v1, hosted at the University of Pretoria (Liesker, 2023).

Glossary

Bounded Weak Echo Region (BWER) - A vertical column of weak radar reflectivity that is bounded by higher reflectivity above and on both sides (in the mid-levels). It is an indication of a strong updraft within a thunderstorm.

Doppler velocity - The radial component of velocity of a scattering object.

Highveld - Elevated area of 1500 m above mean sea level and greater located over the eastern interior of South Africa.

Hook Echo - A pendent, hook or similar shaped echo in reflectivity in the lower levels caused by precipitation drawn into the rotating updraft of a thunderstorm.

Mesocyclone - Cyclonic rotating vortex within a thunderstorm (supercell) that has a diameter between 1 and 10 km and extends between 2 and 8 km above the ground.

Radar reflectivity - More accurately known as the radar reflectivity factor or equivalent radar reflectivity factor. The amount of power scattered back by a radar target (e.g., rain and hail), and depends on the size, shape, aspect, amount, and dielectric properties of the target.

Supercell - Fairly long-lived, often severe type of thunderstorm that contains a deep and persistent rotating updraft.

Weak Echo Region (WER) - A vertical column of weak radar reflectivity that is bounded by higher reflectivity above and on one side.

References

Admirat, P., Goyer, G. G., Wojtiw, L., Carte, E. A., Roos, D. & Lozowki, E. P., 1985. A comparative study of hailstorms in Switzerland, Canada and South Africa. J. Clim. 5(1), 35-51. https://doi.org/10.1002/joc.3370050104.

Antonescu, B., Carbunaru, D., Sasu, M., Burcea, S. & Bell, A., 2010. A Climatology of supercells in Romania. *In:* Proceedings of the 6th European Conference on Radar in Meteorology and Hydrology: Advances in Radar Technology (ERAD2010), 6-10 September 2010. Sibiu, Romania.

Blamey, R. C., Middleton, C., Lennard, C. & Reason, C. J. C., 2017. A climatology of potential severe convective environments across South Africa. Clim. Dyn. 49(5), 2161-2178. https://doi.org/10.1007/s00382-016-3434-7.

Bluestein, H. B. & Woodall, G. R., 1990. Doppler-Radar Analysis of a Low-Precipitation Severe Storm. Mon. Weather Rev. 118(8), 1640-1665. https://doi.org/10.1175/1520-0493(1990)118<1640:DRAOAL>2.0.CO;2.

Brooks, H. E., Lee, J. W. & Craven, J. P.,2003. The spatial distribution of severe thunderstorm and tornado environments from global reanalysis data. Atmos. Res. 67, 73-94. https://doi.org/10.1016/S0169-8095(03)00045-0.

Brown, R. A. & Wood, V. T., 2007. A Guide for Interpreting Doppler Velocity Patterns: Northern Hemisphere Edition. NOAA/National Severe Storms Laboratory.

Brown, R. A., Wood, V. T. & Sirmans, D., 2002. Improved tornado detection using simulated and actual WSR-88D data with enhanced resolution. J. Atmos. Ocean. Technol. 19(11), 1759-1771. https://doi.org/10.1175/1520-0426(2002)019<1759:ITDUSA>2.0.CO;2.

Browning, K. A.,1964. Airflow and Precipitation Trajectories Within Severe Local Storms Which Travel to the Right of the Winds. J. Atmos. Sci. 21(6), 634-639. https://doi.org/10.1175/1520-0469(1964)021<0634:AAPTWS>2.0.CO;2.

Bunkers, M. J., Hjelmfelt, M. R. & Smith, P. L., 2006. An Observational Examination of Long-Lived Supercells. Part I: Characteristics, Evolution, and Demise. Weather Forecast. 21(5), 673-688. https://doi.org/10.1175/WAF949.1.

Bunkers, M. J., Klimowski, B. A., Zeitler, J. W., Thompson, R. L. & Weisman, M. L., 2000. Predicting Supercell Motion Using a New Hodograph Technique. Weather Forecast. 15(1), 61-79. https://doi.org/10.1175/1520-0434(2000)015<0061:PSMUAN>2.0.CO;2.

Burgess, D. W. & Davies-Jones, R. P., 1979. Unusual Tornadic Storms in Eastern Oklahoma on 5 December 1975. Mon. Weather Rev. 107(4), 451-457. https://doi.org/10.1175/1520-0493(1979)107<0451:UTSIEO>2.0.CO;2.

Burgess, D. W. & Lemon, L. R., 1990. Severe Thunderstorm Detection by Radar, in: Atlas, D. (ed.) Radar in Meteorology: Battan Memorial and 40th Anniversary Radar Meteorology Conference. American Meteorological Society, Boston, pp. 619-647.

Carte, A. E., 1979. Sustained Storms on the Transvaal Highveld. S. Afr. Geogr. J. 61(1), 39-56. https://doi.org/10.1080/03736245.1979.10559604.

Carte, A. E., 1981. Morphology of Persistent Storms in the Transvaal on 16/17 October 1978. Beitr. Phys. Atmos 54(1), 86-100.

Carte, A. E. & Held, G., 1978. Variability of Hailstorms on the South African Plateau. J. Appl. Meteorol. 17(3), 365-373. http://www.jstor.org/stable/26178012.

Christodoulou, M. & Sioutas, M., 2017. Radar Climatology of Supercell Thunderstorms in Northern and Central Greece, in: Karacostas, T., Bais, A. & Nastos, P. (eds), Perspectives on Atmospheric Sciences. Springer, Cham, pp. 247-253.

Davies-Jones, R., 1984. Streamwise vorticity: The origin of updraft rotation in supercell storms. J. Atmos. Sci. 41(20), 2991-3006. https://doi.org/10.1175/1520-0469(1984)041<2991:SVTOOU>2.0.CO;2.

De Coning, E. & Adam, B. F., 2000. The tornadic thunderstorm events during the 1998-1999 South African summer. Water SA 26(3), 361-376. https://wrcwebsite.azurewebsites.net/wp-content/uploads/mdocs/WaterSA_2000_03_1263.pdf.

De Coning, E., Adam, E. & Benitz, B. F., 2000. A severe weather event on 29 December 1997: Synoptic and mesoscale perspectives. Water SA 26(2), 137-146. https://journals.co.za/content/waters/26/2/AJA03784738_2344.

Dixon, M. & Wiener, G., 1993. TITAN: Thunderstorm Identification, Tracking, Analysis, and Nowcasting—A Radar-based Methodology. J. Atmos. Ocean. Technol. 10, 785-797. https://doi.org/10.1175/1520-0426(1993)010<0785:TTITAA>2.0.CO;2

Donaldson, R. J., 1970. Vortex Signature Recognition by a Doppler Radar. J. Appl. Meteorol. 9(4), 661-670. https://doi.org/10.1175/1520-0450(1970)009<0661:VSRBAD>2.0.CO;2.

Doswell III, C. A. & Schultz, D. M., 2006. On the Use of Indices and Parameters in Forecasting Severe Storms. Electro. J. Severe Storms Meteorol. 1(3). https://doi.org/10.55599/ejssm.v1i3.4.

Dyson, L. L., Heerden, J. v. & Sumner, P. D., 2015. A baseline climatology of sounding-derived parameters associated with heavy rainfall over Gauteng, South Africa. Int. J. Climatol. 35(1), 114-127. https://doi.org/10.1002/joc.3967.

Dyson, L. L., Pienaar, N., Smit, A. & Kijko, A., 2021. An ERA-Interim HAILCAST hail climatology for southern Africa. Int. J. Climatol. 41(1), 262-277. https://doi.org/10.1002/joc.6619.
Falk, K. W. 1997. Techniques for Issuing Severe Thunderstorm and Tornado warnings with the WSR-88D Doppler Radar. Technical Memorandum, SR-185. NOAA.
Feldmann, M., Germann, U., Gabella, M. & Berne, A., 2021. A characterisation of Alpine mesocyclone occurrence. Weather Clim. Dyn. 2(4), 1225-1244. https://doi.org/10.5194/wcd-2-1225-2021.
Goliger, A. & Lunt, B. G., 1997. Inkanyamba: tornadoes in South Africa, CSIR, Building Technology :Weather Bureau, South Africa.
Goliger, A. M. & Retief, J. V., 2007. Severe wind phenomena in Southern Africa and the related damage. J. Wind Eng. Ind. Aerodyn. 95(9), 1065-1078. https://doi.org/10.1016/j.jweia.2007.01.029.
Grant, L. D. & van den Heever, S. C.,2014. Microphysical and Dynamical Characteristics of Low-Precipitation and Classic Supercells. J. Atmos. Sci. 71(7), 2604-2624. https://doi.org/10.1175/JAS-D-13-0261.1.
Held, G. & Carte, A. E., 1979. Hailstorms in the Transvaal During January 1975. S. Afri. Geogr. J. 61(2), 128-142. https://doi.org/10.1080/03736245.1979.10559613.
Hocker, J. E. & Basara, J. B., 2008. A Geographic Information Systems–Based Analysis of Supercells across Oklahoma from 1994 to 2003. J. Appl. Meteorol. Climatol. 47(5), 1518-1538. https://doi.org/10.1175/2007JAMC1673.1.
Howard, E. & Washington, R., 2019. Drylines in southern Africa: Rediscovering the Congo air boundary. J. Climate 32(23), 8223-8242. https://doi.org/10.1175/JCLI-D-19-0437.1.
Joe, P. & May, P. T., 2003. Correction of Dual PRF Velocity Errors for Operational Doppler Weather Radars. J. Atmos. Ocean. Technol. 20(4), 429-442. https://doi.org/10.1175/1520-0426(2003)20<429:CODPVE>2.0.CO;2.
Johns, R. H. & Doswell III, C. A.,1992. Severe Local Storms Forecasting. Weather Forecast. 7(4), 588-612. https://doi.org/10.1175/1520-0434(1992)007<0588:SLSF>2.0.CO;2.
Klemp, J. B. & Wilhelmson, R. B., 1978. The Simulation of Three-Dimensional Convective Storm Dynamics. J. Atmos. Sci. 35(6), 1070-1096. https://doi.org/10.1175/1520-0469(1978)035<1070:TSOTDC>2.0.CO;2.
Klimowski, B. A., Bunkers, M. J., Hjelmfelt, M. R. & Covert, J. N., 2003. Severe Convective Windstorms over the Northern High Plains of the United States. Weather Forecast. 18(3), 502. https://doi.org/10.1175/1520-0434(2003)18<502:SCWOTN>2.0.CO;2.
Kruger, A., Rae, K. & McBride, C., 2018. Summary of 2017 Climate and Significant Weather Events. South African Weather Service, Pretoria. http://www.weathersa.co.za/Documents/Corporate/Newsletter_May.pdf (accessed 28 January 2020).
Lekoloane, L. E., Bopape, M.-J. M., Rambuwani, T. G., Ndarana, T., Landman, S., Mofokeng, P., Gijben, M. & Mohale, N., 2021. A dynamic and thermodynamic analysis of the 11 December 2017 tornadic supercell in the Highveld of South Africa. weather Clim. Dyn. 2(2), 373-393. https://doi.org/10.5194/wcd-2-373-2021.
Lemon, L. R., 1977. New Severe Thunderstorm Radar Identification Techniques and Warning Criteria: A preliminary report. Kansas City, Missouri: U.S. Department of Commerce, National Oceanic and Atmospheric Administration, National Weather Service. https://apps.dtic.mil/dtic/tr/fulltext/u2/a099510.pdf (accessed 19 February 2020).
Liesker, C. G., 2021. Characteristics of warm season supercell thunderstorms over the Gauteng and Mpumalanga Provinces of South Africa. MSc Dissertation, University of Pretoria. http://hdl.handle.net/2263/83956.
[dataset] Liesker, C. G., 2023. Radar-derived supercell thunderstorm database over the Gauteng and Mpumalanga provinces of South Africa from the warm seasons of 2010/2011 until 2019/2020. University of Pretoria. https://doi.org/10.25403/UPresearchdata.23617092.v1.

Mader, G. N., Neishlos, H., Saunders, M. M. & Carte, A. E., 1986. Some characteristics of storms on the transvaal highveld. J. Clim. 6(2), 173-182. https://doi.org/10.1002/joc.3370060206.
Markowski, P. M.,2002. Hook Echoes and Rear-Flank Downdrafts: A Review. Mon. Weather Rev. 130(4), 852-876. https://doi.org/10.1175/1520-0493(2002)130<0852:HEARFD>2.0.CO;2.
Moller, A. R., Doswell III, C. A., Foster, M. P. & Woodall, G. R., 1994. The Operational Recognition of Supercell Thunderstorm Environments and Storm Structures. Weather Forecast. 9(3), 327-347. https://doi.org/10.1175/1520-0434(1994)009<0327:TOROST>2.0.CO;2.
Mulholland, J. P., Nesbitt, S. W., Trapp, R. J., Rasmussen, K. L. & Salio, P. V., 2018. Convective storm life cycle and environments near the Sierras de Córdoba, Argentina. Mon. Weather Rev. 146(8), 2541-2557. https://doi.org/10.1175/MWR-D-18-0081.1.
Ndarana, T., Rammopo, T. S., Reason, C. J., Bopape, M.-J., Engelbrecht, F. & Chikoore, H., 2022. Two types of ridging South Atlantic Ocean anticyclones over South Africa and the associated dynamical processes. Atmos. Res. 265, 105897. https://doi.org/10.1016/j.atmosres.2021.105897.
Olivier, J., 1990. Hail in the Transvaal: Some Geographical and climatological aspects. PhD Thesis, University of Johannesburg. https://hdl.handle.net/10210/11151.
Piscitelli, F. M., Ruiz, J. J., Negri, P. & Salio, P., 2022. A multiyear radar-based climatology of supercell thunderstorms in central-eastern Argentina. Atmos. Res. 277, 106283. https://doi.org/10.1016/j.atmosres.2022.106283.
Powell, C. L. & Burger, R. P., 2014. The severe Gauteng hailstorms of 28 November 2013. *In:* 30th Conference of South African Society for Atmospheric Sciences, 1 - 2 October 2014, Potchefstroom, South Africa. SASAS. http://dspace.nwu.ac.za/handle/10394/16144?show=full (accessed 29 May 2020).
Prociv, K. A., 2012. Terrain and landcover effects of the southern Appalachian Mountains on the low-level rotational wind fields of supercell thunderstorms. MSc Dissertation, Virginia Tech. http://hdl.handle.net/10919/32463.
Rae, K. J., 2014. A modified Supercell Composite Parameter for supercell thunderstorms over the Gauteng Province, South Africa. Msc Dissertation, University of Pretoria. http://hdl.handle.net/2263/45918.
Rauber, R. M. & Nesbitt, S. W., 2018. Radar Meteorology: A First Course, John Wiley & Sons, Hoboken, NJ.
Ray, P., 1990. Convective Dynamics, in: Atlas, D. (ed.) Radar in Meteorology: Battan Memorial and 40th Anniversary Radar Meteorology Conference. American Meteorological Society, Boston, MA, pp. 348-390.
Simpson, L.-a. & Dyson, L. L., 2018. Severe weather over the Highveld of South Africa during November 2016. Water SA 44(1), 75-85-85. https://doi.org/10.4314/wsa.v44i1.09.
Singleton, A. & Reason, C., 2007. Variability in the characteristics of cut-off low pressure systems over subtropical southern Africa. Int. J. Climatol. 27(3), 295-310. https://doi.org/10.1002/joc.1399.Steyn, R. T. & Bruintjes, P. C. L. a., 1990. Convective cloud characteristics for the Bethlehem area. Water SA 16(2), 115-118. https://hdl.handle.net/10520/AJA03784738_2208.
Stumpf, G. J., Witt, A., Mitchell, E. D., Spencer, P. L., Johnson, J. T., Eilts, M. D., Thomas, K. W. & Burgess, D. W., 1998. The National Severe Storms Laboratory Mesocyclone Detection Algorithm for the WSR-88D. Weather Forecast. 13(2), 304-326. https://doi.org/10.1175/1520-0434(1998)013<0304:TNSSLM>2.0.CO;2.
Taljaard, J. J., 1996. Synoptic climatology and weather phenomena of South Africa. Part 6 Rainfall in South Africa. South African Weather Bureau, Technical Paper No. 32, 89.
Taszarek, M., Allen, J. T., Marchio, M. & Brooks, H. E.,2021. Global climatology and trends in convective environments from ERA5 and rawinsonde data. npj Clim. Atmos. Sci 4(1), 1-11. https://doi.org/10.1038/s41612-021-00190-x.

Tyson, P., Garstang, M., Swap, R., Kallberg, P. & Edwards, M., 1996. An air transport climatology for subtropical southern Africa. Int. J. Climatol. 16(3), 265-291. https://doi.org/10.1002/(SICI)1097-0088(199603)16:3<265::AID-JOC8>3.0.CO;2-M.
Tyson, P. D. & Preston-Whyte, R. A., 2000. The Weather and Climate of Southern Africa, Oxford University Press, Oxford, New York.
U. S. Geological Survey, 2000. *EROS Archive - Digital Elevation - Shuttle Radar Topography Mission (SRTM) Non-Void Filled*. https://doi.org/10.5066/F7K072R7 (accessed 18 March 2021).
Van Schalkwyk, L., Blamey, R., Dyson, L. & Reason, C., 2022. A climatology of drylines in the interior of subtropical southern Africa. J. Climate 35(19), 6411-6430. https://doi.org/10.1175/JCLI-D-21-1005.1.
Van Schalkwyk, L., Blamey, R. C., Gijben, M. & Reason, C. J., 2023. A Climatology of Dryline-Related Convection on the Western Plateau of Subtropical Southern Africa. J. Geophys. Res. Atmos. 128(18), 1-21. https://doi.org/10.1029/2023JD038966.
Wapler, K., Hengstebeck, T. & Groenemeijer, P., 2016. Mesocyclones in Central Europe as seen by radar. Atmos. Res. 168, 112-120. https://doi.org/10.1016/j.atmosres.2015.08.023.
Weisman, M. L. & Klemp, J. B., 1984. The Structure and Classification of Numerically Simulated Convective Storms in Directionally Varying Wind Shears. Mon. Weather Rev. 112(12), 2479-2498. https://doi.org/10.1175/1520-0493(1984)112<2479:TSACON>2.0.CO;2.
Weisman, M. L. & Klemp, J. B., 1986. Characteristics of Isolated Convective Storms, in: Ray, P. S. (ed.) Mesoscale Meteorology and Forecasting. American Meteorological Society, Boston, pp. 331-358.
Wilhelmson, R. B. & Klemp, J. B., 1978. A Numerical Study of Storm Splitting that Leads to Long-Lived Storms. J. Atmos. Sci. 35(10), 1974-1986. https://doi.org/10.1175/1520-0469(1978)035<1974:ANSOSS>2.0.CO;2.
Zrnić, D., Burgess, D. & Hennington, L., 1985. Automatic detection of mesocyclonic shear with Doppler radar. J. Atmos. Ocean. Technol. 2(4), 425-438. https://doi.org/10.1175/1520-0426(1985)002<0425:ADOMSW>2.0.CO;2.